Desalination and Water Treatment
www.deswater.com

doi: 10.5004/dwt.2018.22189

121 (2018) 14–21
July

Entropy generation analysis of Cu–water nanofluid flow over a moving wedge

M. Shanmugapriya[a,b,*], P. Sangeetha[a,b]

[a]*Department of Mathematics, SSN College of Engineering, Chennai – 603 110, India,*
emails: shanmugapriyam@ssn.edu.in (M. Shanmugapriya), sangeethap@ssn.edu.in (P. Sangeetha)
[b]*Department of Civil Engineering, SSN College of Engineering, Chennai – 603 110, India*

Received 23 February 2018; Accepted 20 March 2018

ABSTRACT

The boundary layer heat transfer and entropy generation of Cu–water nanofluid over a moving wedge in the presence of thermal radiation have been analyzed. The governing partial differential equations were converted into nonlinear differential equations by using a suitable similarity transformation, which are solved numerically using the shooting technique together with Runge–Kutta fourth order integration scheme. The effective thermal conductivity and viscosity of the nanofluid are approximated by the Maxwell–Garnetts and Brinkman models, respectively. This investigation is compared with other numerical methods and found to have excellent agreement. The velocity and temperature profiles are obtained for different governing parameters such as Prandtl number Pr, the radiation parameters *R*, moving wedge parameters λ and solid volume fraction of the nanofluid φ. In addition, the effect of various physical parameters on the entropy generation number and Bejan number are also analyzed in this investigation.

Keywords: Nanofluid; Thermal radiation; Boundary layer flow; Heat transfer; Entropy analysis

1. Introduction

Nanotechnology has been widely used in many industrial applications. Nanofluids are engineered colloids made of a base fluid and nanoparticles. Nanofluids have remarkable thermophysical properties that make them potentially useful in many heat transfer applications, including electronic cooling systems, fuel cells, engine cooling/vehicle thermal management, solar thermal collectors, domestic refrigerators, chillers, and heat exchangers. The term nanofluid was coined by Choi [1]. The boundary layer flow over a static or moving wedge in nanofluid has been considered by Yacob et al. [2], which is an extension of the flow over a static wedge considered by Falkner and Skan [3]. Shanmugapriya and Chandrasekar [4] analyzed the problem of free and forced convection with suction and injection over a non-isothermal wedge. Kameswaran et al. [5] investigated heat and mass transfer from an isothermal wedge in nanofluids with Soret effect. Salem et al. [6] investigated the problem of boundary layer flow of a Cu–water-based nanofluid over a moving wedge. Xu and Chen [7] presented the effect of variable viscosity and the phenomenon of flow separation, the magnetohydrodynamics (MHD) Cu/Ag–water nanofluids through a permeable wedge. They found that dual solutions exist for negative pressure gradient. Kasmani et al. [8] numerically studied the Soret and Dufour effects on the double-diffusive convective boundary layer flow of a nanofluid past a moving wedge in the presence of suction. The results showed that the heat transfer rate increases on increasing the Soret parameter and it decreases on increasing the Dufour parameter. The mass transfer behaves oppositely to heat transfer.

* Corresponding author.

Presented at the 3rd International Conference on Recent Advancements in Chemical, Environmental and Energy Engineering, 15–16 February, Chennai, India, 2018.

Entropy generation has been studied several decades for ensuring optical thermal systems in contemporary industrial and technological fields such as heat exchangers, geothermal systems, and electronic cooling to name a few. All thermal systems confront with entropy generation. Entropy generation is a criterion of the destruction of the available system work. The evaluation of the entropy generation is carried out to improve system performance. Different sources such as heat transfer, mass transfer and viscous dissipation are responsible for the generation of entropy. Bejan [9] investigated the entropy generation in flow systems and stated that the engineering design of a thermal system could be improved through minimization of entropy production. Bejan [10] presented a method named entropy generation minimization to measure and optimize the disorder or disorganization generated during a process.

Many researchers have developed the concept of entropy generation of thermal systems. Malvandi et al. [11] analytically studied the steady two-dimensional boundary layer flow over an isothermal flat plate by homotopy perturbation method and analyzed the entropy generation inside the boundary layer. Butt et al. [12] have presented the entropy analysis of magnetohydrodynamic flow and heat transfer over a convectively heated radially stretching surface. Butt and Ali [13] have carried out the entropy analysis of flow and heat transfer caused by a moving surface. Butt et al. [14] have studied the effects of thermal radiation and viscous dissipation on entropy generation in the Blasius flow. Rashidi et al. [15] have analyzed the entropy generation in steady MHD flow due to a rotating porous disk in a nanofluid. Ellahi et al. [16] investigated a particle shape factor on natural convection boundary layer flow of a nanofluid over an inverted vertical cone embedded in a porous medium in the presence of MHD, radiation and power law index effects.

Common working fluids in heat transfer industry such as water, ethylene glycol, and engine oil have low thermal conductivities compared with solids. For example, thermal conductivity of copper is 670 times greater than thermal conductivity of water at 25°C. And also Cu–water nanofluid exhibits a better thermal performance among the other considered nanofluids. Therefore, the present study reports the results of boundary layer heat transfer of Cu–water nanofluid over a moving wedge in the presence of thermal radiation. Effects of entropy generation number and Bejan number are also analyzed for various parameters and are presented graphically.

2. Problem formulation

Consider a steady two-dimensional laminar boundary layer flow of an incompressible viscous nanofluid (Cu–water) of density ρ_{nf} and temperature T_∞ moving over a wedge moving with the velocity $u_w(x)$. Choose the co-ordinate system such that x-axis is along the surface of the wedge and y-axis normal to the surface of the wedge. Further it is assumed that the velocity of ambient fluid is $u_e(x) = U_0 x^m$ and the velocity of the moving wedge is $u_w(x) = U_w x^m$, where U_0, U_w and m are all constant with $0 \le m \le 1$. Here $m = \beta/(2-\beta)$, where β is the Hartree pressure gradient parameter that corresponds to $\beta = \Omega/\pi$ for the total wedge angle Ω. Thermal radiation is included in the energy equation. The governing equations for this case can be written (Tiwari and Das [17]) as follows:

$$\frac{\partial u}{\partial x}+\frac{\partial v}{\partial y}=0 \tag{1}$$

$$u\frac{\partial u}{\partial x}+v\frac{\partial u}{\partial y}=u_e(x)\frac{\partial u_e(x)}{\partial x}+\frac{\mu_{nf}\partial^2 u}{\rho_{nf}\partial y^2} \tag{2}$$

$$u\frac{\partial T}{\partial x}+v\frac{\partial T}{\partial y}=\alpha_{nf}\frac{\partial^2 T}{\partial y^2}-\frac{1}{\left(\rho c_p\right)_{nf}}\frac{\partial q_r}{\partial y} \tag{3}$$

subject to the boundary conditions

$$u = u_w(x) = U_w x^m,\ v = 0,\ T = T_w \text{ at } y = 0 \tag{4}$$

$$u = u_e(x) = U_0 x^m,\ T \to T_\infty \text{ as } y \to \infty \tag{5}$$

here u and v are the velocity components along x and y axes, respectively, T is the temperature of the nanofluid in the boundary layers, μ_{nf} is the viscosity of the nanofluid, ρ_{nf} is the density of the nanofluid, α_{nf} is the thermal diffusivity of the nanofluid and $(\rho c_p)_{nf}$ is the heat capacitance of the nanofluid which are defined as follows:

$$\mu_{nf}=\frac{\mu_f}{(1-\phi)^{2.5}},\quad \rho_{nf}=(1-\phi)\rho_f+\phi\rho_S,\quad \alpha_{nf}=\frac{k_{nf}}{\left(\rho c_p\right)_{nf}}$$
$$\left(\rho c_p\right)_{nf}=(1-\phi)\left(\rho c_p\right)_f+\phi\left(\rho c_p\right)_S,\frac{k_{nf}}{k_f}=\frac{\left(k_S+2k_f\right)-2\varphi\left(k_f-k_S\right)}{\left(k_S+2k_f\right)+2\varphi\left(k_f-k_S\right)} \tag{6}$$

where ϕ is the solid volume fraction of the nanofluid, μ_f is the viscosity of the fluid fraction, ρ_f is the reference density of the fluid fraction, ρ_s is the reference density of the solid fraction, k_f is the thermal conductivity of the fluid and k_s is the thermal conductivity of the solid fraction.

Making use of the Rosseland approximation for radiation for an optically thick layer (Brewster [19]), we have:

$$q_r=\frac{-4\sigma}{3k^*}\frac{\partial T^4}{\partial y} \tag{7}$$

where σ is the Stefan–Boltzmann constant and k^* is the mean absorption coefficient. If temperature differences within the flow are sufficiently small such that T^4 may be expressed as a linear function of the temperature, then the Taylor series for T^4 about T_∞ after neglecting higher order terms, is given by:

$$T^4 \cong 4T_\infty^3 T - 3T_\infty^4 \tag{8}$$

In view of Eqs. (7) and (8), Eq. (3) reduces to:

$$u\frac{\partial T}{\partial x}+v\frac{\partial T}{\partial y}=\alpha_{\mathrm{nf}}\frac{\partial^2 T}{\partial y^2}+\frac{16\sigma T_\infty^3}{3k^*\left(\rho c_p\right)_{\mathrm{nf}}}\frac{\partial^2 T}{\partial y^2} \tag{9}$$

We now look for similarity variables of Eqs. (2) and (3) with boundary conditions represented by Eqs. (4) and (5) in the following form (Pal et al. [20]):

$$\begin{aligned}\psi&=\left[\frac{2\nu_f x u_e(x)}{(m+1)}\right]^{1/2} f(\eta),\\ \eta&=\left[\frac{(m+1)u_e(x)}{2\nu_f x}\right]^{1/2} y,\quad \theta(\eta)=\frac{T-T_\infty}{T_w-T_\infty}\end{aligned} \tag{10}$$

where ν_f is the kinematic viscosity of the fluid and the stream function ψ is defined in the usual way as $u=\frac{\partial\psi}{\partial y}$, $v=-\frac{\partial\psi}{\partial x}$ which identically satisfies Eq. (1).

Substituting Eqs. (6) and (10) into Eqs. (2), (4), (5) and (9), we get the following nonlinear ordinary differential equations:

$$f'''+\phi_4\left[ff''+\left(\frac{2m}{m+1}\right)\left(1-f'^2\right)\right]=0 \tag{11}$$

$$\left(1+\frac{4}{3R}\right)\theta''+\mathrm{Pr}\frac{\phi_3}{\phi_5}\left[f\theta'\right]=0 \tag{12}$$

subject to the boundary conditions

$$f(\eta)=0,\ f'(\eta)=\lambda,\ \theta(\eta)=1 \text{ at } \eta=0 \tag{13}$$

$$f'(\eta)=1,\ \theta(\eta)=0 \text{ as } \eta\to\infty \tag{14}$$

where prime denotes differentiation with respect to η, Pr is the Prandtl number, R is the radiation parameter and λ is the ratio of the wall velocity to the free stream fluid velocity. They are, respectively, defined as:

$$\mathrm{Pr}=\frac{\nu_f}{\alpha_f},\quad R=\frac{k_{\mathrm{nf}}k^*}{4\sigma T_\infty^3},\quad \lambda=\frac{U_w}{U_0} \tag{15}$$

Also, we have

$$\phi_1=(1-\phi)^{2.5},\ \phi_2=1-\phi+\phi\left(\frac{\rho_s}{\rho_f}\right),\quad \phi_3=1-\phi+\phi\frac{\left(\rho c_p\right)_s}{\left(\rho c_p\right)_f} \tag{16}$$

$$\phi_4=(1-\phi)^{2.5}\left[1-\phi+\phi\frac{\left(\rho c_p\right)_s}{\left(\rho c_p\right)_f}\right],\quad \phi_5=\frac{k_{\mathrm{nf}}}{k_f}. \tag{17}$$

The physical quantities of the skin friction coefficient and the Nusselt number are calculated, respectively, by the following equations:

$$C_f=\frac{\tau_w}{\rho_f\left[u_e(x)\right]^2},\quad \mathrm{Nu}_x=\frac{q_w x}{k_f\left(T_w-T_\infty\right)} \tag{18}$$

where $\tau_w=\mu_{\mathrm{nf}}\left(\frac{\partial u}{\partial y}\right)_{y=0}$ is the wall shear stress, and $q_w=-k_{\mathrm{nf}}\left(\frac{\partial T}{\partial y}-q_r\right)_{y=0}$ is the local heat flux.

Using the new similarity variables in Eq. (10) gives:

$$\begin{aligned}\mathrm{Re}_x^{1/2}C_f&=\frac{(m+1)}{2(1-\phi)^{2.5}}f''(0),\\ \mathrm{Re}_x^{-1/2}\,\mathrm{Nu}_x&=\frac{-k_{\mathrm{nf}}}{k_f}\left(\frac{2}{m+1}\right)\left(1+\frac{4}{3R}\right)\theta'(0)\end{aligned} \tag{19}$$

where $\mathrm{Re}_x=u_e(x)x/\nu_f$ is the local Reynolds number. Table 1 shows the thermo physical properties of fluid and nanoparticles given by Oztop and Abu-nada [18].

2.1. Numerical modelling

Eqs. (11) and (12) along with the boundary conditions represented by Eqs. (13) and (14) constitute a two point boundary value problem. These equations are solved using shooting method, by converting them to an initial value problem. For this, we convert the non-linear ordinary differential equations (Eqs. (11) and (12)) into a system of first-order differential equations as follows:

$$u_1'=u_2,\ u_2'=u_3,\ u_3'=-\phi_4\left[u_1u_3+\left(\frac{2m}{m+1}\right)\left(1-u_2^2\right)\right] \tag{20}$$

$$v_1'=v_2,\ v_2'=-\mathrm{Pr}\frac{\phi_3}{\phi_5}\frac{1}{\left(1+\frac{4}{3R}\right)}\left[u_1v_2\right] \tag{21}$$

where $u_1=f$, $u_2=f'$, $u_3=f''$, $v_1=\theta$ and $v_2=\theta'$.

The boundary conditions (Eqs. (13) and (14)) become:

$$u_1(0)=0,\ u_2(0)=\lambda,\ u_3(0)=\alpha_1,\ v_1(0)=0,\ v_2(0)=\alpha_2 \tag{22}$$

Table 1
Thermophysical properties of fluid and nanoparticle (Oztop and Abu-nada [18])

Physical properties	Fluid phase (water)	Cu
c_p (J/kg K)	4,179	385
ρ (kg/m^3)	997.1	8,933
κ (W/m K)	0.613	400
$\alpha\times10^{-7}$ (m^2/s)	1.47	1,163.1

To solve Eqs. (20) and (21) as an initial value problem, the values of $u_3(0)$ and $v_2(0)$ are required. But no such values are given at the boundary. So the suitable guess values for $u_3(0)$ and $v_2(0)$ are chosen and the fourth order Runge–Kutta method with step size 0.001 is applied to obtain the solution. The computations have been carried out for different values of m, Prandtl number Pr, the radiation parameters R, moving wedge parameters λ and solid volume fraction of the nanofluid ϕ. An accuracy of 10^{-5} is restricted for the sake of convergence.

2.2. Entropy generation analysis

The local volumetric rate of entropy generation for a viscous incompressible conducting fluid in the presence of thermal radiation is defined (Arpaci [21] and Woods [22]) as follows:

$$S'''_{\text{gen}} = \underbrace{\frac{1}{T^2}\left[k_{\text{nf}}\left(\frac{\partial T}{\partial y}\right)^2 + \frac{16\sigma T_\infty^3}{3k^*}\left(\frac{\partial T}{\partial y}\right)^2\right]}_{\text{HFI}} + \underbrace{\left[\frac{\mu_{\text{nf}}}{T}\left(\frac{\partial u}{\partial y}\right)^2\right]}_{\text{FFI}} \tag{23}$$

In Eq. (23), HFI is the heat transfer irreversibility due to heat transfer in the direction of finite temperature gradients and FFI is the contribution of fluid friction irreversibility to the local entropy generation. The first term on the right-hand side of Eq. (23) is the local entropy generation due to heat transfer, the second term is the local entropy generation due to radiation, the third term is the local entropy generation due to viscous dissipation.

It is appropriate to determine dimensionless number for entropy generation rate S'''_{gen}. We obtained the entropy generation number by division of the local volumetric entropy generation rate to a S'''_{gen} characteristic rate of entropy generation S_{Go}. The characteristic entropy generation rate is:

$$\bar{S}'''_{\text{gen}} = \frac{S'''_{\text{gen}}}{S_{\text{Go}}} \tag{24}$$

The characteristic entropy generation rate is:

$$S_{\text{Go}} = \frac{k_{\text{nf}}\left(T_w - T_\infty\right)^2 u_e(x)^2}{T^2 \nu_f^2} \tag{25}$$

Using the definition of ψ in Eq. (10), the velocity and temperature derivative can be expressed as:

$$\frac{\partial u}{\partial y} = u_e(x) f''(\eta)\left[\frac{(m+1)u_e(x)}{2\nu_f x}\right]^{1/2},$$
$$\frac{\partial T}{\partial y} = \left(T_w - T_\infty\right)\theta'(\eta)\left[\frac{(m+1)u_e(x)}{2\nu_f x}\right]^{1/2} \tag{26}$$

Substituting Eqs. (23), (25) and (26) into Eq. (24), the entropy generation equation for Cu–water nanofluid over a moving wedge can be expressed as:

$$\bar{S}'''_{\text{gen}} = \left(\frac{m+1}{2}\right)\frac{1}{\text{Re}_x}\left[\left(1+\frac{4}{3R}\right)(\theta')^2 + \frac{\text{Pr}\,\text{Ec}\,\Omega}{(1-\phi)^{2.5}}\left(\frac{k_f}{k_{\text{nf}}}\right)(f'')^2\right] \tag{27}$$

where $\Omega = \frac{T}{T_w - T_\infty}$ is the dimensionless temperature difference, $\text{Re}_x = \frac{u_e(x)x}{\nu_f}$ is the local Reynolds number and $\text{Ec} = \frac{u_e(x)^2}{(c_p)_f\left(T_w - T_\infty\right)}$ is the Eckert number.

The Bejan number Be is defined to be the ratio of entropy generation due to heat transfer to the entropy generation:

$$\text{Be} = \frac{\text{Entropy generation due to heat transfer}}{\text{Entropy generation number}} = \frac{\text{HFI}}{\text{HFI} + \text{FFI}} \tag{28}$$

The Bejan number Be takes the values between 0 and 1. The value of Bejan number is more/less than 0.5 shows that the contribution of HFI to the total entropy generation is higher/less than that of FFI. The limiting value of Be = 1 shows that the active entropy generation mechanism is HFI while Be = 0 represents no HFI contribution to the total entropy production.

3. Results and discussion

3.1. Effect of parameter variation on velocity and temperature profiles

Figs. 1 and 2 show the effect of the velocity ratio parameters λ on velocity and temperature profiles for $R = 1$, $\phi = 0.1$ and $m = 1$, respectively. These figures shows that there are regions of unique solutions for $\lambda > -1$ and dual solutions for $\lambda_c < \lambda \le -1$. The velocity profiles for unique solution increases with increasing value of λ. The first solution of velocity profiles exhibit the identical characters as that of the velocity profiles for unique solution and reverse nature is noticed for the case of the second solution. From Fig. 2, it is noticed that the temperature profiles for first solution decreases for an increase of λ and it decreases for the second solution also the unique solution of temperature profiles is similar to the profiles of the first solution.

Figs. 3 and 4 represent the velocity and temperature profiles at $\lambda = 1.2$ and $\lambda = -1.2$ for different values of radiation parameters R. From Fig. 3, it is observed that the radiation parameter has a negligible effect on the velocity profiles. When $\lambda = 1.2$ there is only a unique solution and the temperature profiles are decreasing with an increase of radiation parameter, the different behaviour appears when $\lambda = -1.2$. The temperature profile of the first solution increases with an increase in R within the thermal boundary layer and the reverse is seen away from the surface. Also it is observed that, far away from the surface, the temperature profile for the second solution exhibit the identical characters as that of the first solution. For $\lambda = -1.2$, the temperature inside the boundary layer for the first solution is high for large value of R, while outside the boundary layer, the temperature is low with large value of R. For the second solution the behaviour is similar, far away from the surface.

The effects of volume fraction of nanoparticles φ on velocity and temperature profiles at $\lambda = 1.2$ and $\lambda = -1.2$ with $R = 1$ and $m = 1$ are shown in Figs. 5 and 6. It can be seen that the decrease in ϕ decrease in momentum boundary layer for the first and second solution. For the unique solution, the behaviour is opposite. Also it is noted that the increase of ϕ decrease in thermal boundary layer for first and second solution. The contrary behaviour has been observed for unique solution.

3.2. Effects of parameter variation on entropy generation number and Bejan number

Fig. 7 demonstrates the effect of m on the entropy generation number. It is observed that entropy generation increases with increasing m. The effect of the Prandtl number Pr on $\bar{S}'''_{gen}$ is shown in Fig. 8, which shows that an increase in Pr results is an increase of the entropy generation rate near the surface. But the inverse behaviour is observed away from the surface. Fig. 9 shows the effect of the Eckert number Ec on the local entropy generation number and it is noticed that entropy generation increases with increasing Ec. Similar trend is observed in Fig. 10, the values of $\bar{S}'''_{gen}$ increases with an increasing value of the dimensionless temperature difference Ω.

In Figs. 11–13, the Began number is displayed as a function of λ. From these figures, it can be seen that the Bejan number decreases near the velocity ratio parameter ($-1 \le \lambda \le 0.2$) and increases afterwards by decreasing values of Pr, Ec and Ω.

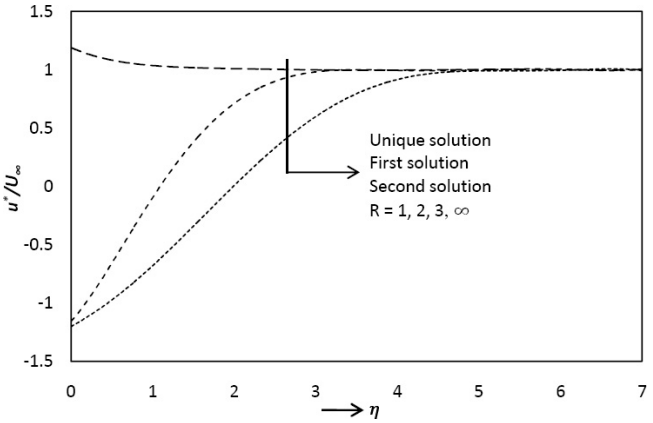

Fig. 3. Velocity profile for different values of R when φ = 0.1 and $m = 1$.

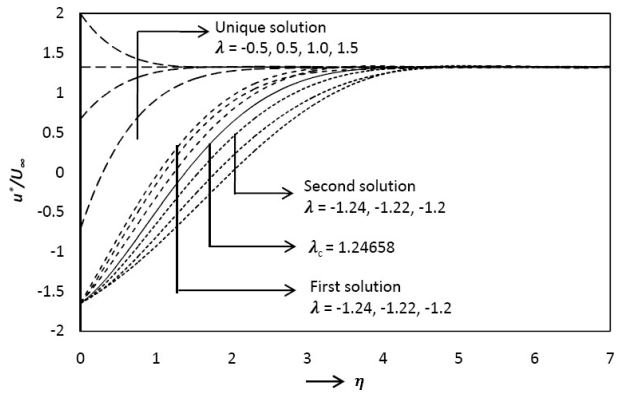

Fig. 1. Velocity profile for different values of λ when $R = 1$, φ = 0.1 and $m = 1$.

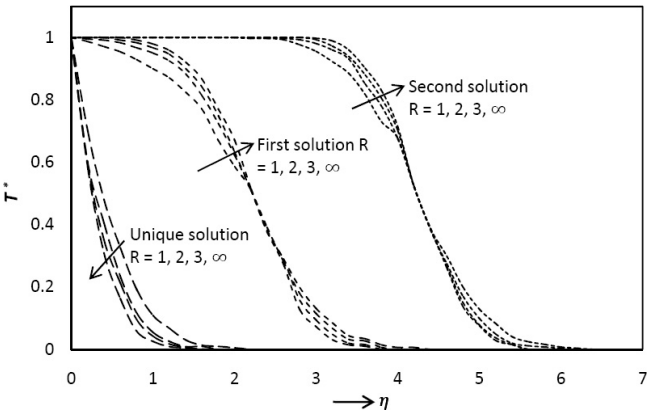

Fig. 4. Temperature profile for different values of R when φ = 0.1 and $m = 1$.

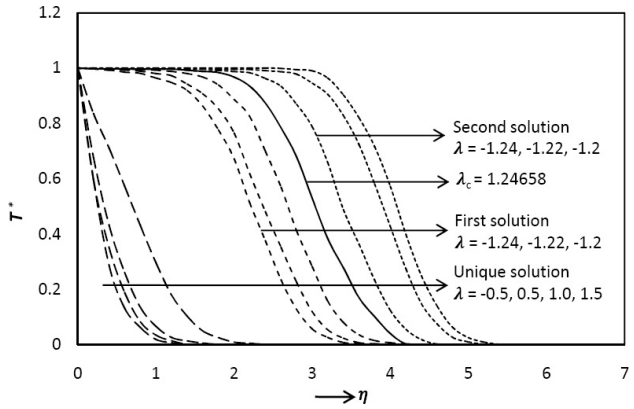

Fig. 2. Temperature profile for different values of λ when $R = 1$, φ = 0.1 and $m = 1$.

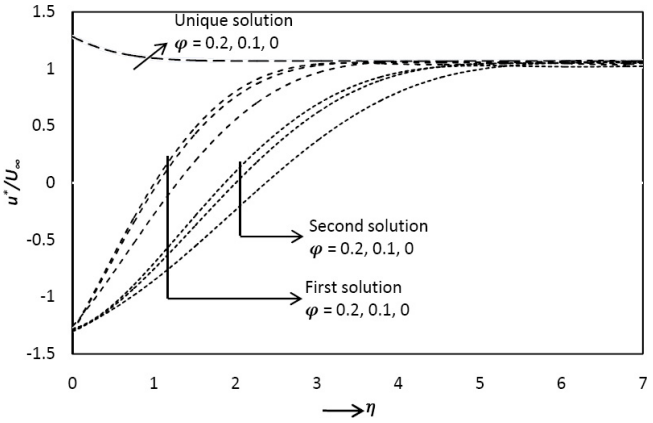

Fig. 5. Velocity profile for different values of φ when $R = 1$ and $m = 1$.

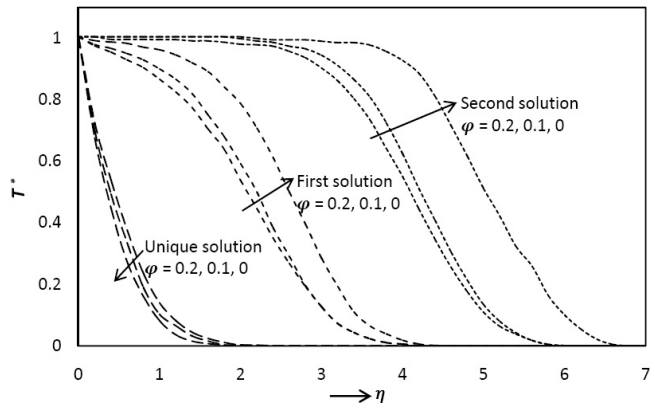

Fig. 6. Temperature profile for different values of φ when $R = 1$ and $m = 1$.

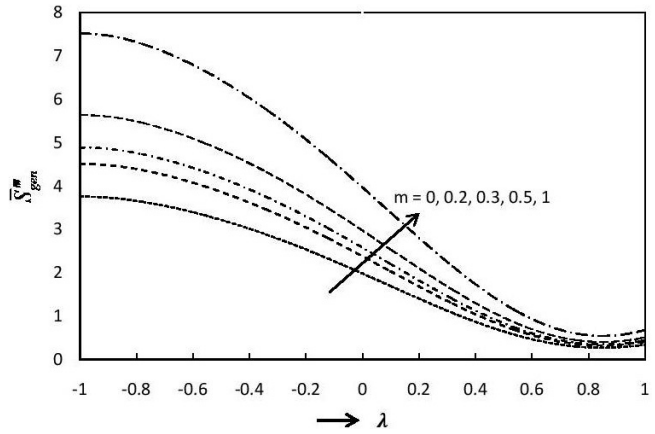

Fig. 7. Effect of m on the local entropy generation number.

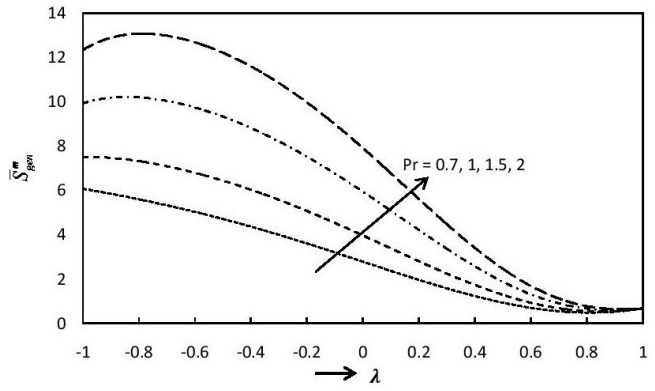

Fig. 8. Effect of Prandtl number on the entropy generation number.

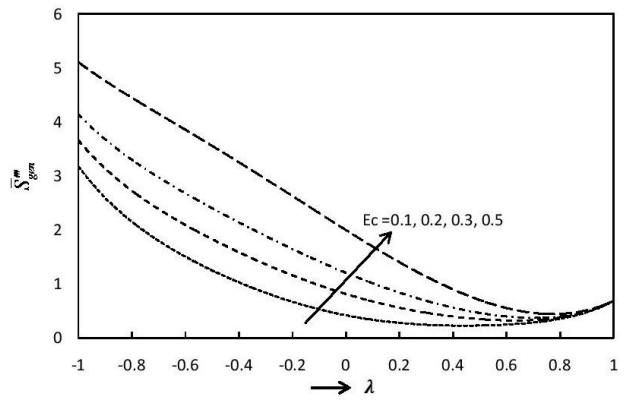

Fig. 9. Effect of the Eckert number on the entropy generation number.

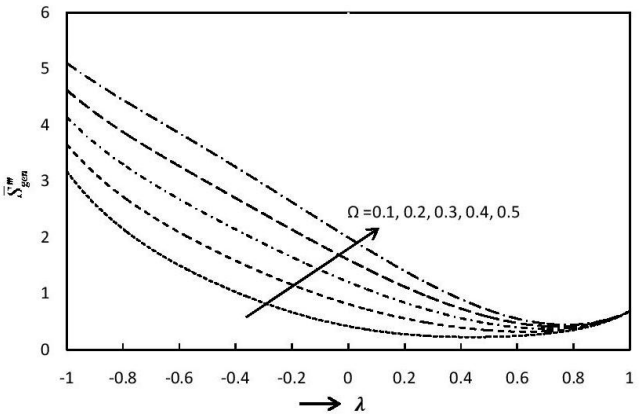

Fig. 10. Effect of Ω on the entropy generation number.

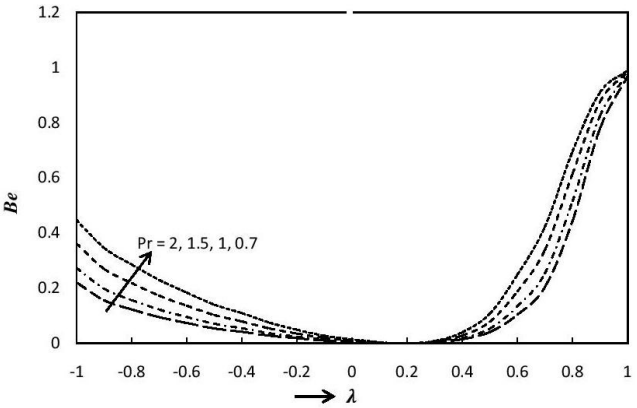

Fig. 11. Effect of Prandtl number on the Bejan number.

4. Conclusion

In the present study, the effects of thermal radiation on entropy generation of Cu–water nanofluid flow over a moving wedge are investigated. The velocity and temperature profiles are obtained numerically and used to compute the entropy generation number. The effects of m, the Prandtl number Pr, the radiation parameters R, moving wedge parameters λ and solid volume fraction of the nanofluid ϕ on velocity and temperature profiles are presented. The influences of the same parameters on the entropy generation rate and Bejan number are also discussed. It is observed that there is an increase in the entropy generation number $\bar{S}_{gen}'''$ with increasing m, Prandtl number Pr, Eckert number Ec and the dimensionless temperature difference Ω. The Bejan number decreases near the velocity ratio parameter and increases afterwards by decreasing values of Pr, Ec and Ω.

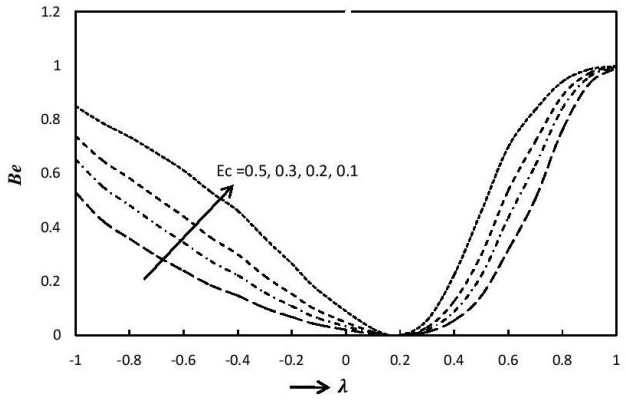

Fig. 12. Effect of the Eckert number on the Bejan number.

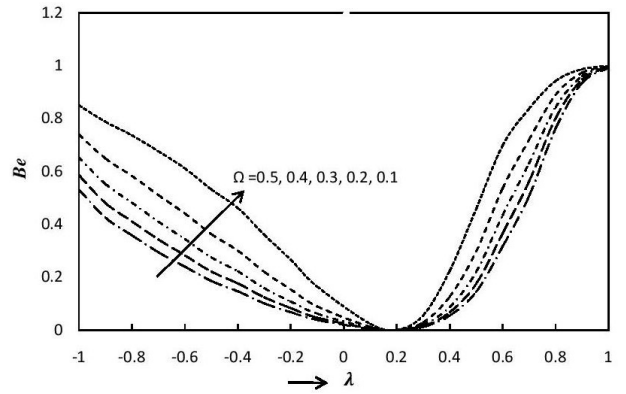

Fig. 13. Effect of Ω on the Bejan number.

Symbols

C_f	—	Skin friction coefficient
Nu_x	—	Local Nusselt number
Re_x	—	Local Reynolds number
τ_w	—	Wall shear stress
q_w	—	Local heat flux
$\bar{S}'''_{gen}$	—	Volumetric entropy generation rate
u, v	—	Velocity components along x and y axes, respectively
T	—	Fluid temperature
f	—	Dimensionless stream function
Pr	—	Prandtl number
R	—	Radiation parameters
λ	—	Moving wedge
ϕ	—	Solid volume fraction of the nanofluid
Ω	—	Dimensionless temperature difference
Ec	—	Eckert number
Be	—	Bejan number

Greek

μ_{nf}	—	Viscosity of the nanofluid
ρ_{nf}	—	Density of the nanofluid
α_{nf}	—	Thermal diffusivity of the nanofluid
$(\rho c_p)_{nf}$	—	Heat capacitance of the nanofluid
μ_f	—	Viscosity of the fluid fraction
ν_f	—	Kinematic viscosity of the fluid
ρ_f	—	Density of the fluid fraction
ρ_s	—	Density of the solid fraction
k_f	—	Thermal conductivity of the fluid
k_s	—	Thermal conductivity of the solid fraction
σ	—	Stefan–Boltzmann constant
k^*	—	Mean absorption coefficient
ψ	—	Stream function
θ	—	Dimensionless temperature

Subscripts

∞	—	Free stream condition
0	—	Temperature at the wall

Acknowledgement

The authors would like to thank the Management of SSN College of Engineering for providing the necessary facility to carry out the present work.

References

[1] S.U.S. Choi, Enhancing Thermal Conductivity of Fluids with Nanoparticles, Proceedings, ASME International Mechanical Engineering Congress and Exposition, ASME, FED 231/MD, San Francisco, CA, USA, 1995, pp. 99–105.
[2] N.A. Yacob, A. Ishak, I. Pop, Falkner-Skan problem for a static or moving wedge in nanofluids, Int. J. Thermal Sci., 50 (2011) 133–139.
[3] V.M. Falkner, S.W. Skan, Some approximate solutions of boundary layer equations, Philos. Mag., 12 (1931) 865–896.
[4] M. Shanmugapriya, M. Chandrasekar, Analytic solution of free and forced convection with suction and injection over a non-isothermal wedge, Bull. Malays. Math. Sci. Soc., 31 (2008) 11–24.
[5] K. Kameswaran, M. Narayana, S. Shaw, P. Sibanda, Heat and mass transfer from an isothermal wedge in nanofluids with Soret effect, Eur. Phys. J. Plus, 129 (2014) 154–164.
[6] F.A. Salama, Effect of radiation on convection heat transfer of Cu-water nanofluid past a moving wedge, Thermal Sci., 20 (2016) 437–447.
[7] X. Xu, S. Chen, Dual solutions of a boundary layer problem for MHD nanofluids through a permeable wedge with variable viscosity, Boundary Value Problems, 2017 (2017) 1–13.
[8] R.M. Kasmani, S. Sivasankaran, M. Bhuvaneswari, A.K. Hussein, Analytical and numerical study on convection of nanofluid past a moving wedge with Soret and Dufour effects, Int. J. Num. Meth. Heat Fluid Flow, 27 (2017) 2333–2354.
[9] A. Bejan, A study of entropy generation in fundamental convective heat transfer, J. Heat Transfer, 101 (1979) 718–725.
[10] A. Bejan, Entropy Generation Minimization, 2nd ed., CRC, Boca Raton, Florida, USA, 1996.
[11] A. Malvandi, D. Ganji, F. Hedayati, M.H. Kaffash, M. Jamshidi, Series solution of entropy generation toward an isothermal flat plate, Thermal Sci., 16 (2012) 1289–1295.
[12] A.S. Butt, A. Ali, Entropy analysis of magnetohydrodynamic flow and heat transfer over a convectively heated radially stretching surface, J. Taiwan Inst. Chem. Eng., 45 (2014) 1197–1203.
[13] A.S. Butt, A. Ali, Entropy analysis of flow and heat transfer caused by a moving plate with thermal radiation, J. Mech. Sci. Technol., 28 (2014) 343–348.
[14] A.S. Butt, S. Munawar, A. Ali, A. Mehmood, Entropy generation in the Blasius flow under thermal radiation, Phys. Scr., 85 (2012) 1–6.
[15] S. Rashidi, N. Abelman, M. Freidooni, Entropy generation in steady MHD flow due to a rotating porous disk in a nanofluid, Int. J. Heat Mass Transfer, 62 (2013) 515–525.
[16] R. Ellahi, M. Hassan, A. Zeeshan, Shape effects of nanosize particles in Cu—H_2O nanofluid on entropy generation, Int. J. Heat Mass Transfer, 81 (2015) 449–456.

[17] R.K. Tiwari, M.K. Das, Heat transfer augmentation in a two-sided lid-driven differentially heated square cavity utilizing nanofluids, Int. J. Heat Mass Transfer, 50 (2007) 2002–2018.
[18] H. Oztop, E. Abu-Nada, Numerical study of natural convection in partially heated rectangular enclosures filled with nanofluids, Int. J. Heat Fluid Flow, 29 (2008) 1326–1336.
[19] M.Q. Brewster, Thermal Radiative Transfer Properties, Wiley, New York, 1972.
[20] D. Pal, G. Mandal, K. Vajravelu, MHD convection-dissipation heat transfer over a non-linear stretching and shrinking sheets in nanofluids with thermal radiation, Int. J. Heat Mass Transfer, 65 (2013) 81–90.
[21] V.S. Arpaci, Radiative entropy production-lost heat into entropy, Int. J. Heat Mass Transfer, 30 (1987) 2115–2123.
[22] L.C. Woods, Thermodynamics of Fluid Systems, Oxford University Press, Oxford, 1975.